DOI: 10.1007/s11099-016-0230-x PHOTOSYNTHETICA 55 (1): 58-68, 2017

Leaf *vs*. inflorescence: differences in photosynthetic activity of grapevine

M. SAWICKI[+], B. COURTEAUX, F. RABENOELINA, F. BAILLIEUL, C. CLEMENT, E. AIT BARKA, C. JACQUARD[#], and N. VAILLANT-GAVEAU[#]

Université de Reims Champagne-Ardenne, UFR Sciences Exactes et Naturelles, SFR Condorcet FR CNRS 3417, Unité de Recherche Vignes et Vins de Champagne - EA 4707, Laboratoire de Stress, Défenses et Reproduction des Plantes, Moulin de la Housse - Bâtiment 18, BP 1039, 51687 REIMS Cedex 2, France

Abstract

Using measures of gas exchange and photosynthetic chain activity, we found some differences between grapevine inflorescence and leaf in terms of photosynthetic activity and photosynthesis regulations. Generally, the leaf showed the higher net photosynthesis (P_N) and lower dark respiration than that of the inflorescence until the beginning of the flowering process. The lower (and negative) P_N indicated prevailing respiration over photosynthesis and could result from a higher metabolic activity rather than from a lower activity of the photosynthetic apparatus. Considerable differences were observed between both organs in the functioning and regulation of PSI and PSII. Indeed, in our conditions, the quantum yield efficiency and electron transport rate of PSI and PSII were higher in the inflorescence compared to that of the leaf; nevertheless, protective regulatory mechanisms of the photosynthetic chain were clearly more efficient in the leaf. This was in accordance with the major function of this organ in grapevine, but it highlighted also that inflorescence seems to be implied in the whole carbon balance of plant. During inflorescence development, the global PSII activity decreased and PSI regulation tended to be similar to the leaf, where photosynthetic activity and regulations remained more stable. Finally, during flowering, cyclic electron flow (CEF) around PSI was activated in parallel to the decline in the thylakoid linear electron flow. Inflorescence CEF was double compared to the leaf; it might contribute to photoprotection, could promote ATP synthesis and the recovery of PSII.

Additional key words: cyclic electron flow; chlorophyll fluorescence; gas exchange; inflorescence; photosystem; *Vitis vinifera*.

Introduction

Although leaves are traditionally considered as the main source of photosynthates, reproductive structures, such as green flowers or developing fruits, are also photosynthetically active and therefore can assimilate substantial amounts of carbon in many plants (Weiss *et al*. 1988, Blanke and Lenz 1989, Abdel-Reheem *et al*. 1991). Net photosynthesis was measured in reproductive structures of many species, in both sterile and fertile parts of the inflorescence, such as calyx lobes (Yonemori *et al*. 1996), bracts (Werk and Ehleringer 1983, Heilmeier and Whale 1987), sepals (Dueker and Arditti 1968, Kirichenko *et al*. 1989), anthers (Keijzer and Willemse 1988, Kirichenko *et al*. 1993, Clément *et al*. 1997a), corolla (Clément *et al*. 1997b), capsules (Dogane and Ando 1990) or flower stalks (Jurik 1985). Flower photosynthesis may supply a significant fraction of the total carbon and cover a part of reproduction energy costs (Bazzaz *et al*. 1979, Reekie and Bazzaz 1987, Marcelis and Hofman-Eijer 1995, Antlfinger and Wendel 1997). Indeed in woody species, analysis of the reproduction carbon consumption in several deciduous

Received 3 February 2016, *accepted* 4 April 2016, *published as online-first* 21 April 2016.
[+]Corresponding author; e-mail: me.sawicki@laposte.net
Abbreviations: BBCH – Biologische Bundesanstalt, Bundessortenamt and Chemical Industry; CEF – cyclic electron flow; Chl – chlorophyll; cyt b_6f – cytochrome b_6f complex; DS – developmental stage; ETR_I – electron transport rate of PSI; ETR_{II} – electron transport rate of PSII; F_0 – minimal fluorescence yield of the dark-adapted state; F_0' – minimal fluorescence yield of the light-adapted state; F_m – maximal fluorescence yield of the dark-adapted state; F_m' – maximal fluorescence yield of the light-adapted state; Fd – ferredoxin; FNR – ferredoxin $NADP^+$ reductase; FM – fresh mass; F_v/F_m – maximum quantum yield of PSII photochemistry; NPQ – nonphotochemical quenching; LEF – linear electron flow; PC – plastocyanin; PEPC – phospho*enol*pyruvate carboxylase; P_N – net photosynthetic rate; PQ – plastoquinone; R_D – dark respiration; ROS – reactive oxygen species; RuBP – ribulose-1,5-bisphosphate; Y_{CEF} – quantum yield of cyclic electron flow; Y_I – efficient quantum yield of PSI; Y_{II} – efficient quantum yield of PSII; Y_{NA} – PSI acceptor side limitation; Y_{ND} – PSI donor side limitation; Y_{NO} – quantum yield of nonregulated energy dissipation; Y_{NPQ} – quantum yield of regulated energy dissipation.
[#] These authors contributed equally to this project and should be considered coauthors.

trees highlighted that flower photosynthesis supplies 2.3% (*Quercus macrocarpa*) to 64.5% (*Acer platanoides*) of total carbon required for the production of mature seeds (Bazzaz *et al*. 1979). The photosynthetic contribution by green reproductive structures in relation to their own carbon requirement varies and depends on the ambient conditions, the species, and the type of organ (Marcelis and Hofman-Eijer 1995). For instance, apple flowers contribute significantly to carbohydrate balance (15–33%) during the flowering and fruit setting periods (Vemmos and Goldwin 1994). Finally, photosynthetic activity of reproductive organs significantly enhances fruit yield in a number of crop species (Sawicki *et al*. 2015a, Weiss *et al*. 1990) and reduces the cost of reproduction (Aschan and Pfanz 2003).

In grapevine (*Vitis vinifera* L.), inflorescence contains chlorophyll (Chl) from bud burst until berry ripening (Palliotti and Cartechini 2001, Lebon *et al*. 2005a, 2008). The inflorescences of Gewurztraminer and Pinot noir grapevine cultivars have shown variations in the photosynthetic activity during flower development (Lebon *et al*. 2005a, Sawicki *et al*. 2015b). More recently, it was demonstrated that the inflorescence is able to assimilate and distribute carbon during flower development, mainly to vegetative organs until flower blooming (Vaillant-Gaveau *et al*. 2011). Carbohydrate physiology in inflorescence is poorly understood up to the flowering stage. In the grapevine flower, female meiosis coincides with drastic physiological changes in the whole plant. At this time, carbon nutrition switches from the mobilization of wood reserves to photosynthesis in the leaves (Lebon *et al*. 2004, Zapata *et al*. 2004a,b). While leaf photosynthesis activity has been largely studied in grapevine under field and stress conditions (Bertamini and Nedunchezhian 2002, Bertamini *et al*. 2005), scarce information is available on inflorescence. It was only shown that grapevine inflorescence is able to respond to UV (Petit *et al*. 2009) and to cold stress (Sawicki *et al*. 2012, 2015b,c) by adapting its defense and carbohydrate metabolism, respectively.

The light reactions of photosynthesis convert light energy into chemical energy (ATP and NADPH). Linear electron flow (LEF) is mediated by the two photosystems and generates both ATP and NADPH. Cyclic electron flow (CEF) around PSI preferentially generates ATP without the accumulation of NADPH in chloroplasts (Shikanai 2014). It has been proposed that a high CEF may directly dissipate the energy absorbed by PSI (Laisk *et al*. 2010) and two distinct pathways of CEF have been suggested for higher plants. Both pathways involve ferredoxin (Fd) and have been referred to a PGR5–PGRL1 protein-dependent pathway and to a chloroplast NADH dehydrogenase-like complex-dependent pathway. The functioning of these two pathways is suggested to result in the generation of a pH gradient across the thylakoid membrane (ΔpH) which in turn drives the ATP synthesis and may also function to regulate light harvesting, by inducing high energy state quenching (Heber and Walker 1992, Johnson 2011). The CEF induction and regulation are poorly documented (Livingston *et al*. 2010). CEF has been found to be highly active in C_4 plants (Kubicki *et al*. 1996), green algae (Finazzi *et al*. 2002), and cyanobacteria (Carpentier *et al*. 1984). In these species, an 'extra' proton translocation or ATP was presumably needed, especially to run CO_2-concentrating mechanisms. In C_3 plants that do not concentrate CO_2, the LEF alone should nearly meet their ATP demands (Avenson *et al*. 2005). Nevertheless, substantial CEF increase in C_3 plants was observed under stress conditions such as drought (Jia *et al*. 2008) or photosynthetic induction (Joët *et al*. 2002, Joliot and Joliot 2002). More recently, it was finally shown that CEF around PSI was accelerated with the progress of leaf senescence, probably to replenish the ATP and to maintain a satisfactory nonphotochemical energy quenching (Kotakis *et al*. 2014).

The objectives of this study were to assess the gas exchange, the photosynthetic chain activity, and the expression of related genes in grapevine inflorescence and leaf throughout the developmental stages in order to investigate the photosynthetic activity in both organs.

Materials and methods

Plants: Experiments were performed on *Vitis vinifera* L. (cv. Pinot noir) fruiting cuttings obtained from grapevine canes according to the protocol of Sawicki *et al*. (2015b). Developmental stages were identified according to the BBCH (Biologische Bundesanstalt, Bundessortenamt and Chemical Industry) scale (Meier 2001). In inflorescence, analyses were carried out from the female meiosis stage (BBCH 55 + 2 d adapted from works of Lebon *et al*. 2005b) until the fruit-set stage according to seven developmental stages (DS) (*see* the text table).

Six-week-old leaves were used and measurements were performed during the first four days (D1−D4), and after seven (D7) and ten days (D10). Inflorescences and leaves were collected at each developmental stage, frozen in liquid N_2 and stored at −80°C until the determination of gene expression.

Gas exchange: The net photosynthesis (P_N) of inflorescence and leaf were determined simultaneously with an

Developmental stage in BBCH scale	Abbreviation
BBCH 55 + 2 d (ovulary meiosis)	DS1
BBCH 55 + 3 d	DS2
BBCH 55 + 4 d	DS3
BBCH 57 d (flower separating)	DS4
BBCH 60 d (first detached floral caps)	DS5
BBCH 68 d (80% fallen flower hoods)	DS6
BBCH 71 d (fruit set)	DS7

open gas-exchange system (*LI−6400*, *Li−Cor*, Lincoln, USA), using equations developed by von Caemmerer and Farquhar (1981). For the inflorescence experiment, the infrared gas analysis system was equipped with a *6400-22* opaque conifer chamber, while a standard leaf chamber was used for leaves. Photosynthetically active radiation provided by a red-blue light emitting diode (*Li-6400-22L* or *6400-02B Li-Cor*) was fixed at 1,500 µmol(photon) m^{-2} s^{-1}. Air temperature and humidity were maintained at 25°C and 30%, respectively, and the external CO_2 concentration was kept at a constant level of 380 ppm.

The dark respiration (R_D) of both organs was determined simultaneously as net photosynthesis without light.

The same plants were used for all measurements. Five plants were used per treatment and time point and three biological replicates were performed. Separated inflorescences and leaves were collected and weighted at each developmental stage to express the results in gram of fresh mass (FM) allowing the comparison of both organs.

PSI and PSII photochemistry: Chl fluorescence parameters and the redox change of P700 were assessed simultaneously with a *Dual-PAM-100* measuring system (*Heinz Walz*, Germany) on the same plants used for gas-exchange measurements.

PSII photochemistry: Inflorescences and leaves were dark adapted for 30 min in order to determine the minimal level of fluorescence (F_0) and the maximal fluorescence (F_m) after a saturating flash [1 s, 13,000 µmol(photon) m^{-2} s^{-1}]. The ratio of variable to maximal fluorescence [$F_v/F_m = (F_m - F_0)/F_m$] was calculated. Actinic illumination [216 µmol(photon) m^{-2} s^{-1}] was applied and after fluorescence stabilization, a second saturating flash (1 s) was imposed to determine the maximal fluorescence (F_m') of a light-adapted inflorescence. Removal of the actinic light and exposure to a short period of far-red light allowed measurement of the zero level of fluorescence (F_0'). In both dark- and light-adapted states, the fluorescence parameters were calculated according to Genty *et al*. (1989) and Schreiber *et al.* (1994). Quantum yields, designated by Y_{II} [$Y_{II} = (F_m' - F)/F_m'$] for photochemical energy utilization in PSII, Y_{NPQ} for regulated energy dissipation in PSII and Y_{NO} for nonregulated energy dissipation in PSII, were calculated according to Kramer *et al*. (2004). The electron flow through PSII (ETR_{II}) was calculated according to Miyake *et al*. (2005): $ETR_{II} = Y_{II} \times PPFD \times \alpha_{II}$, where α_{II} is the fraction of the incident light absorbed by organ (p) × fraction of the absorbed light distributed to PSII (d_{II}).

PSI photochemistry: Together with fluorescence measurement, the saturation pulse method was used to determine P700 parameters following the method of Klughammer and Schreiber (1994, 2008). The $P700^+$ signals may vary between a minimal (P700 fully reduced, closed) and a maximal level (P700 fully oxidized). P700 fully oxidized (P_m) was determined by application of a saturation pulse after far-red pre-illumination. Y_{NA}, the quantum yield of nonphotochemical energy dissipation due to acceptor-side limitation, was calculated based on a P_m' determination at actinic light of 216 µmol(photon) m^{-2} s^{-1} according to: $Y_{NA} = (P_m - P_m')/P_m$. Y_{ND}, the nonphotochemical quantum yield of PSI due to donor-side limitation, was calculated according to: $Y_{ND} = 1 - P700_{red}$. Y_I, the photochemical quantum yield of PSI, was defined by the fraction of overall P700, which is reduced and not limited by acceptor side. Y_I was calculated from the complementary PSI quantum yields of nonphotochemical energy dissipation, Y_{ND}, and Y_{NA} according to: $Y_I = 1 - Y_{ND} - Y_{NA}$. The electron transport rate of PSI, ETR_I, was calculated by *Dual-PAM* software. Y_{CEF}, the yield of cyclic electron flow, was calculated as $Y_{CEF} = Y_I - Y_{II}$ (Huang *et al*. 2010). The relation between CEF and LEF was detected by calculating the changes of the Y_{CEF}/Y_{II} ratio during the developmental process.

Gene expression: For RNA extraction, samples (six pooled plants) were ground with ball mill (30 s, 20 Hz). Depending on the organ, 100 mg (flowers) or 50 mg (leaves) of powder were used for total RNA extraction using *Plant RNA Purification Reagent* (*Invitrogen*, France), according to the manufacturer's instructions. The RNA pellet was resuspended in 20 µl of RNase-free water, flower RNAs were treated with *RQ1* DNase enzyme (*Promega*) and all are quantified by measuring absorbance at 260 nm.

Real-time PCR analysis: Total RNAs (150 ng) were reverse-transcribed using *verso cDNA Synthesis Kit* (*Thermo Fisher Scientific*, France) according to the manufacturer's protocol. Real-time PCR was performed using *Absolute Blue QPCR SYBR Green* (*Thermo Fisher Scientific*, France), in a *CFX96* real-time PCR detection system (*Bio-Rad*, France). The thermal profile was: 10 s at 95°C (denaturation) and 45 s at 60°C (annealing/extension) for 40 cycles. The specificity of PCR amplification was checked using a heat dissociation curve from 65 to 95°C following the final cycle. PCR efficiency of the primer sets was calculated by performing real-time PCR on serial dilutions of cDNA.

For each experiment, PCR reactions were performed in duplicate and three independent experiments were analyzed. *EF1α* and *60RSP* genes were used to normalize our results (Table 1) and relative gene expression was determined with the formula $2^{-\Delta\Delta Ct}$ (Livak and Schmittgen 2001), using *CFX Manager 3.0* software. The first point of kinetic was chosen to represent 1x expression of interest genes (Table 1) and results were expressed as the fold increase of mRNA level over reference sample. Expression of genes encoding PSII proteins (*QB*, *PsbP2*, *PsbS*), PSI protein (*PS1A2*), cytochrome b_6f complex (*Cytb*$_6$*f*), photosynthetic electron transport (*PC*, *Fd*, *FNR*), F-type ATP synthase (*ATPase*), and two genes coding Rubisco (*RbcL,* large and *RbcS,* small subunits) were tracked.

Table 1. Genes, homologies and primer sequences used for real-time qPCR.

Gene	Encoding	Sequences 5'-3'	NBCI accession
EF1-α	Elongation factor 1-alpha	AACCAAAATATCCGGAGTAAAAGA GAACTGGGTGCTTGATAGGC	XM_002284888
60 RSP	60S ribosomal protein L18	ATCTACCTCAAGCTCCTAGTC CAATCTTGTCCTCCTTTCCT	XM_002270599.1
ATPase	ATP synthase gamma chain, chloroplastic-like	CGCGACGGTGATTCAAACTC ACCTTATCCCTCTCCACGCT	XM_002278082.1
Cytb$_6$f	Cytochrome *b*$_6$-*f* complex iron-sulfur subunit	CGGACCCTCACACAAGGATTA CCGAGGTGAGTGCAGACAG	XM_002276734.1
Fd	Ferredoxin	TGTGGATCAGTCTGACGGGA CTCCTCCTCCTTGTGGGTCT	XM_002269581.1
FNR	Ferredoxin NADP reductase	GGCATTGCTCCTTTTCGCTC CGTCCTTGTACAGCAGGGAG	XM_002274330.2
PC	Plastocyanin	TCGATGTCCGAAGAGGATCTG ACCCTGGTGAGGAGAACAGT	XM_002285868.2
PsbP2	Putative oxygen evolving enhancer protein	CAGGCTGCAAACTTCACTCG TCTCCCACCTCCTCTCGTTG	XM_002284220.2
PSIA2	PSI P700 chlorophyll *a* apoprotein A2	AAAGGCGCTTTAGATGCACG ATGCGTCCCAAGCCGAAATA	YP_567075.1
PsbS	PSII 22 kDa protein	AATTGAGGGGGCAGTCATCC TGCCCAACTGAGCCAATCTT	XM_002285821.2
QB	Photosystem Q(B) protein-like PSII P680 reaction center D1 protein	ACAAGCAAGAGCAATCCTTCAG TTTGGATCCGATACGCCTGG	XM_002277124.2
RbcS	Small subunit of Rubisco	GTGCAATGCATCGCTTTCATT TCCACAAGGGTCCTAAACATGAG	TC52496
RbcL	Large subunit of Rubisco	AATTTTTCCTCCACGGCGATA ATCTGCGCCCGCCTTTATA	TC57584

Statistical analysis: All experiments were repeated independently three times and the standard error was shown. Statistical analyses were performed with *STATISTICA* software (p<0.05) using a two-way analysis of variance (*ANOVA*) to compare inflorescence and leaf responses along the experiment. *Student*'s *t*-test was performed with the same software (p<0.05) to analyze gene expression results in each organ.

Results

Gas exchange: In leaf, P_N was about 520 μmol(CO_2) g^{-1}(FM) s^{-1} and remained stable along the experiment (Fig. 1*A*). In inflorescence, P_N was negative for the entire experimental period (Fig. 1*B*). P_N was relatively stable around –21 μmol(CO_2) g^{-1}(FM) s^{-1} from DS1 until DS4. During the flowering process, P_N oscillated by increasing at DS5 [–4.6 μmol(CO_2) g^{-1}(FM) s^{-1}], decreasing at DS6 [–30.2 μmol(CO_2) g^{-1}(FM) s^{-1}], and recovering globally the initial value at DS7 [–17.4 μmol(CO_2) g^{-1}(FM) s^{-1}] (Fig. 1*B*, Table 2).

Along the experiment in leaf, R_D oscillated slightly between 65 and 43 μmol(CO_2) g^{-1}(FM) s^{-1} (Fig. 2*A*). In inflorescence, R_D was significantly higher than that in leaf around 100 μmol(CO_2) g^{-1}(FM) s^{-1} until DS4, (Fig. 2*A*, Table 2). Then, R_D decreased progressively during the floral development to reach the lowest value at DS7 [43 μmol(CO_2) g^{-1}(FM) s^{-1}].

PSII and PSI photochemistry: Activity of PSII: In leaf, F_v/F_m was about 0.81 and always higher than that in flower (Fig. 2*B*) in which F_v/F_m was around 0.77 between DS1 and DS5, with an increase (+2%) at DS2. This parameter decreased at DS6 (–6% at 0.72) and finally increased at DS7 (0.75).

In leaf, ETR_{II} was relatively stable until D7 [between 15 and 20 μmol(e^-) m^{-2} s^{-1}] and decreased slightly at D10 [12.7 μmol(e^-) m^{-2} s^{-1}]. In flower, ETR_{II} was 28.2 μmol(e^-) m^{-2} s^{-1} at DS2; then decreased until DS6 [15.3 μmol(e^-) m^{-2} s^{-1}; Fig. 2*C*] to finally increase at DS7 to 19.3 μmol(e^-) m^{-2} s^{-1}.

In leaf, Y_{NO} was relatively stable around 22% during the experiment. Y_{II} decreased between D1 and D3 (34.1 to 26.7%), increased between D3 and D7 (31.3%), and finally decreased between D7 and D10 (23%). Conversely, Y_{NPQ} increased between D1 and D3 (44.2 to 52.0%), decreased between D3 and D7 (48.4%), and finally increased to reach 53.9% at D10 (Fig. 3*A,* Table 2). In flower, Y_{II} decreased from 51.1 to 27.8% between DS1 and DS6 and increased at DS7 (35.0%; Fig. 3*A*). Y_{NPQ} was 22.7% at DS1 and increased gradually to 32.0% at DS5, then decreased to

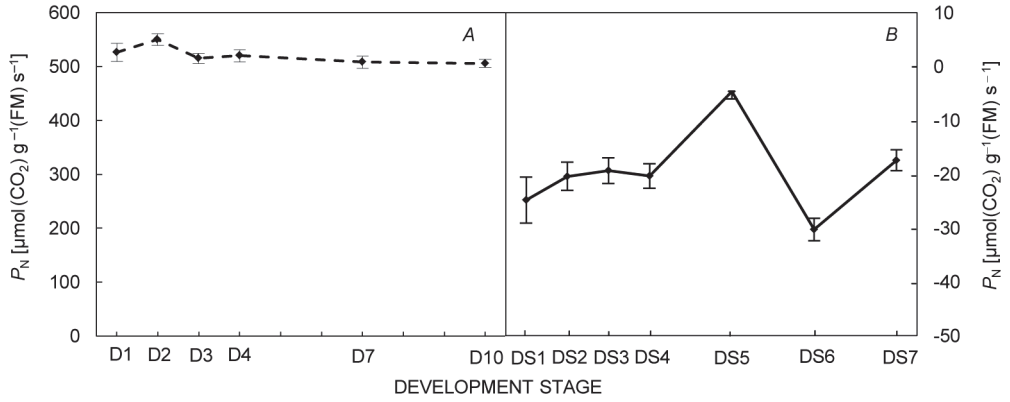

Fig. 1. Changes in net photosynthesis (P_N) in Pinot noir (*A*) leaf and (*B*) inflorescence. In inflorescence, measurements were performed at female meiosis stage (BBCH 55 + 2 d: DS1), one (BBCH 55 + 3 d: DS2), two (BBCH 55 + 4 d: DS3), and three (BBCH 57 d: DS4) days after meiosis and at BBCH 60 (DS5), 68 (DS6) and 71 (DS7) stages. Six-week-old leaves were used and measurements were performed during the first four days (D1–D4), and after seven (D7) and ten days (D10). The mean ± SE was calculated from three independent experiments.

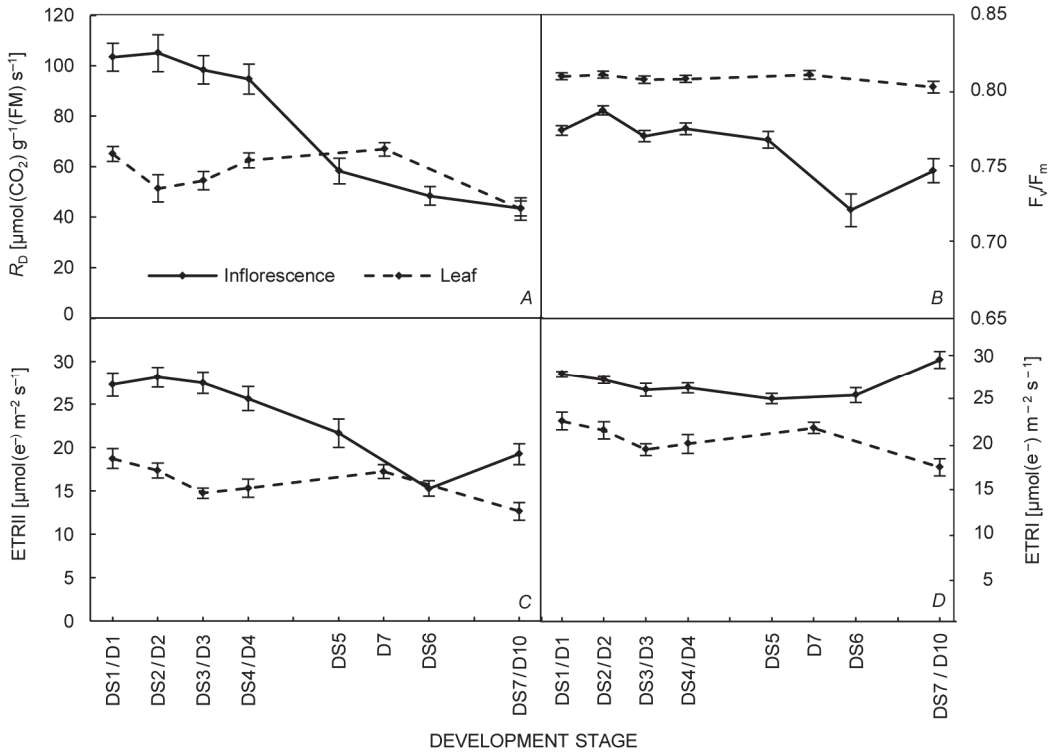

Fig. 2. Changes in (*A*) dark respiration (R_D), (*B*) maximum efficiency of PSII photochemistry after dark adaptation (F_v/F_m), (*C*) rate of charge separation at PSII reaction centers (ETR_{II}), (*D*) rate of charge separation at PSI reaction centers (ETR_I) in Pinot noir flower and leaf. In flower, measurements were performed at female meiosis stage (BBCH 55 + 2 d: DS1), one (BBCH 55 + 3 d: DS2), two (BBCH 55 + 4 d: DS3), and three (BBCH 57 d: DS4) days after meiosis and at BBCH 60 (DS5), 68 (DS6), and 71 (DS7) stages. Six-week-old leaves were used and measurements were performed during the first four days (D1–D4), and after seven (D7) and ten days (D10). The mean ± SE was calculated from three independent experiments.

reach finally 27.5% at DS7 (Fig. 3*A*). Y_{NO} was around 26% in the first stages of development and increased largely at DS6 (42.2%) (Fig. 3*A*).

Finally, we showed that all PSII parameters were significantly different in both organs (Table 2).

Activity of PSI: In leaf, ETR_I was stable and inferior to 24 µmol(e^-) m^{-2} s^{-1} and decreased at D10 (–26.7%) (Fig. 2*D*), whereas in flower, ETR_I was stable around 28 µmol(e^-) m^{-2} s^{-1} during the first stages and increased at fruit set stage (DS7; +16%).

In leaf, Y_I decreased between D1 and D3 (41.7 to 35.8%), increased between D3 and D7 (40.3%), and finally decreased between D7 and D10 to reach 32.1%. Conversely, Y_{ND} increased between D1 and D3 (50.8 to 57.4%), decreased between D3 and D7 (53.2%), and finally increased between D7 and D10 to attain a maximum of 59.9% (Fig. 3*B*). Y_{NA} was relatively stable and low, around 7%, during the experiment. In flower, Y_I remained almost unchanged (varying between 46% and 50%) during the floral development, increasing only at DS7 (54.2%). Y_{ND} was stable during the three first stages, increased between DS3 and DS6 (21.5 to 38.1%), and decreased to 35.8% at DS7. Similar as Y_{ND}, Y_{NA} was stable until DS3 (around 30%), then decreased to reach 12.0% at DS7 (Fig. 3*B*).

In leaf, Y_{CEF} was around 0.1 during the experimental period (Fig. 4*A*). In flower, Y_{CEF} was inactive during the three first stages. It was activated at DS4 (0.02) and was significantly stimulated until DS6 (0.2) and remained stable at DS7 (Fig. 4*A*, Table 2). The ratio of the quantum yield of CEF to Y_{II} [Y_{CEF}/Y_{II}] oscillated between 0.25 and 0.43 during the experiment in leaf. As Y_{CEF}, this ratio was significantly stimulated during the development to reach 0.72 at DS6 (Fig. 4*B*, Table 2).

Photosynthetic gene expression: Besides statistical tests, we decided to consider only genes whose expression presented a two-fold difference. Relative mRNA expression in leaf was consistently higher than that in the inflorescence. In leaf, transcript levels for all tested genes were not significantly modified during the experiment (Fig. 5*A*). In flower, the expression of *PsbP2* gene, encoding PSII protein, was half at DS5, whereas the quantity of *QB* mRNA increased at DS6 (Fig. 5*B*). Expression of genes encoding photosynthetic electron transport proteins (*PC*, *FNR*) decreased at DS5 (–71 and –53%, respectively), similarly as expression of *RbcS* (–70%).

Table 2. Results of a two-way *ANOVA* of photosynthetic parameters with significant results at $P \leq 0.05$ (*), $P \leq 0.01$ (**), $P \leq 0.001$ (***), and not significant (NS), respectively.

Parameter	Organ	Time	Interaction
P_N	***	**	NS
R_D	***	***	***
Y_{II}	***	NS	***
Y_{NO}	***	***	***
Y_{NPQ}	***	***	***
ETR_{II}	***	***	***
F_v/F_m	***	**	NS
Y_I	***	***	***
Y_{NA}	***	***	***
Y_{ND}	***	***	***
ETR_I	***	***	***
Y_{CEF}	NS	***	***
Y_{CEF}/Y_{II}	NS	***	***

Discussion

Photosynthetic activity in leaf and inflorescence: Our data revealed that photosynthesis (photochemical reactions and regulations) is different in both organs and evolves during the inflorescence development. Not surprisingly, the leaf performed a higher net photosynthesis whereas net CO_2 exchange was negative in inflorescence (Fig. 1). The lower P_N in inflorescence could be due to the important respiratory activity (namely until DS4), but should not be due to a low stomatal conductance (data not shown) since its influence is minimal when P_N is negative (efflux).

Although leaves are the major photosynthetic organs, it was suggested that grapevine inflorescences could play a crucial role in nutrient balance by allowing the development of leaves, which in return ensure the carbohydrate availability for their own development (Vaillant-Gaveau *et al*. 2011). As reported in our study, measurements of the gas exchanges of green tomato fruits revealed no net CO_2 fixation whereas Chl fluorescence parameters were similar to those of leaves (Carrara *et al*. 2001). These results can be explained because changes in external CO_2 may not adequately reflect CO_2 uptake in photosynthesis and in particular neglect the amount of internally generated and photosynthetically refixed CO_2 by phospho*enol*pyruvate carboxylase (PEPC; Blanke and Lenz 1989). Concerning grapevine inflorescence, previous experiments highlighted an induction of the *PEPc* gene expression between the female meiosis and the beginning of the flowering process (Sawicki *et al*. 2015c). Finally, a decrease in the expression of both subunits of Rubisco encoding genes (namely *RbcS*) as well as genes encoding some proteins of the photosynthetic chain was observed at DS5, which could be correlated with the drop in P_N measured at DS6 (Figs. 1,5). Indeed, this decrease seems not to be related to the increase in respiration process since we measured a decrease of R_D (Fig. 2).

Different PSII and PSI activity regulations: Our results showed that the activity of the photosynthetic chain highlighted that, in spite of a lower F_v/F_m value, the inflorescence had higher PSII and PSI activities than that of the leaf (Figs. 2*B*, 3). During inflorescence development, global PSII activity decreased. We particularly showed that Y_{II} and Y_{NPQ} had opposite tendency until the beginning of the flowering process, indicating that these parameters are dependent. Y_{NO} increase which was measured thereafter occurred finally due to the decrease in PSII photochemical capacity rather than by the modification in Y_{NPQ} (Fig. 3*A*). Y_{NO} reflects the nonphotochemical quenching other than that caused by the

downregulation of the light-harvesting function, attributable to photoinactivation and nonregulated energy (heat and fluorescence) dissipation of PSII. So, this regulation way is particularly damaging for the photosynthetic chain (Kramer *et al*. 2004, Huang *et al*. 2011). Our results also showed that the total quantum yield of loss increased progressively from the female meiosis stage and was higher than the fraction of energy photochemically converted in PSII. Hence, the photosynthetic performance of the inflorescence decreased during the floral development. This is in accordance with previous works of Lebon *et al*. (2005b) and Vaillant-Gaveau *et al*. (2011) who have respectively shown that the inflorescence Chl content decreases during the floral development process and that the inflorescence is progressively more dependent on leaf photoassimilates for its development.

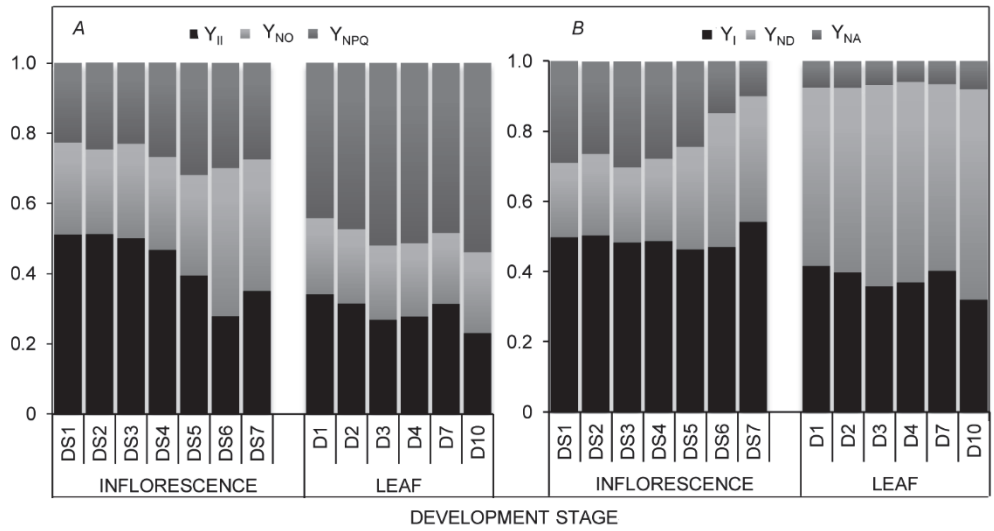

Fig. 3. Changes in (*A*) quantum yield of regulated energy dissipation – Y_{NPQ}, quantum yield of nonregulated energy dissipation – Y_{NO}, and efficient quantum yield of PSII – Y_{II}, (*B*) PSI acceptor side limitation – Y_{NA}, PSI donor side limitation – Y_{ND}, and efficient quantum yield of PSI – Y_I in Pinot noir flower and leaf. In flower, measurements were performed at female meiosis stage (BBCH 55 + 2 d: DS1), one (BBCH 55 + 3 d: DS2), two (BBCH 55 + 4 d: DS3), and three (BBCH 57 d: DS4) days after meiosis and at BBCH 60 (DS5), 68 (DS6), and 71 (DS7) stages. Six-week-old leaves were used and measurements were performed during the first four days (D1–D4), and after seven (D7) and ten days (D10). The mean ± SE was calculated from three independent experiments.

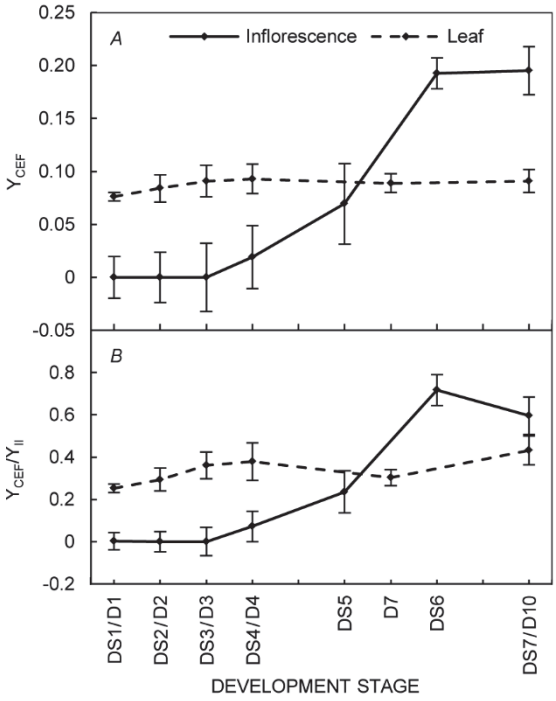

Fig. 4. Changes in (*A*) quantum yield of cyclic electron flow – Y_{CEF}, (*B*) ratio of the quantum yield of CEF to the LEF – Y_{CEF}/Y_{II} in Pinot noir flower and leaf. In flower, measurements were performed at female meiosis stage (BBCH 55 + 2 d: DS1), one (BBCH 55 + 3 d: DS2), two (BBCH 55 + 4 d: DS3), and three (BBCH 57 d: DS4) days after meiosis and at BBCH 60 (DS5), 68 (DS6), and 71 (DS7) stages. Six-week-old leaves were used and measurements were performed during the first four days (D1–D4), and after seven (D7) and ten days (D10). The mean ± standard error was calculated from three independent experiments.

In leaf, Y_{NO} was relatively stable during the experiment while Y_{II} and Y_{NPQ} showed a global and opposite tendency to that in the young inflorescence (until the beginning of the flowering process). So, the PSII photochemistry capacity of the leaf and the young inflorescence depended particularly on the quantum yield of regulated energy dissipation Y_{NPQ}. The relatively high Y_{NPQ} value, namely in leaf, showed that the photon flux density was excessive, but it was regulated to protect itself by the thermal dissipation of excessive excitation energy (Fig. 3*A*) (Kramer *et al*. 2004). Y_{NPQ} could be stimulated by the xanthophyll cycle when excitation energy is in excess.

Without such dissipation, a formation of singlet O_2 and reactive oxygen species could intervene and consequently might cause an increase of Y_{NO}. The low and stable Y_{NO} values in leaf indicated that there was no increased excitation pressure in PSII reaction centers. Therefore, according to Klughammer and Schreiber (2008), these results suggest that protective regulatory mechanisms were more efficient in leaf than in inflorescence during the floral development.

Concerning the PSI functioning, Y_I and Y_{ND} showed a global and opposite tendency during the experiment in leaf. A particularly interesting result was the very low value of the acceptor-side limitation throughout the entire experiment (7% on average). So, in leaf, PSI activity was principally dependent on the PSII activity (donor side) since inhibition of Y_{II} decreased the fraction of reduced PSII electron acceptors and then increased Y_{ND}. Concerning inflorescence, Y_I remained almost unchanged during the floral development but the PSI regulation evolved with an increase of the donor-side limitation and consequently with the decrease of the acceptor-side limitation. The Y_{ND} increase was also consistent with the decrease in PC transcripts measured in flower at DS5 (Figs. 3*B*, 5*B*). Thus, the nonphotochemical quantum yield of PSI was modified during the floral development and PSI electron transfer regulation mode tended to be similar to the leaf's by the end of the experimental period. Y_{NA} represents the over-reduction of the PSI acceptor side, contributing to the PSI photoinhibition. A lower Y_{NA} during development indicated that PSI is well protected against photoinhibition (Golbeck 1987, Golbeck and Bryant 1991). Finally, our results clearly showed that leaf was well protected but also that the inflorescence set up a better protection.

Induction of CEF: In inflorescence, Y_{II} was supplemented with CEF during the flowering process, which appeared at DS4 and was maximal and superior to leaf at DS6 and DS7. Y_{CEF} was stimulated in inflorescence when F_v/F_m, Y_{II}, and ETR_{II} decreased, leading to a Y_{CEF}/Y_{II} increase (Fig. 4). The decrease in Y_{II} can lead to a light energy excess, inducing the generation of ROS. In order to dissipate harmlessly excess light energy as heat, plants must activate NPQ. Previous studies have reported that CEF is necessary for energy dissipating function (Munekage *et al*. 2002, 2004, Nandha *et al*. 2007, Takahashi *et al*. 2009). Moreover, it has been reported that inhibition of Y_{II} and stimulation of CEF are two main mechanisms for the photoprotection of PSI (Sonoike 1995, Munekage *et al*. 2004, Nandha *et al*. 2007, Takahashi *et al*. 2009). In our case, NPQ and CEF were measured simultaneously in leaf whereas in inflorescence, NPQ decreased when CEF was activated. CEF activation in inflorescence might contribute to photoprotection but could also

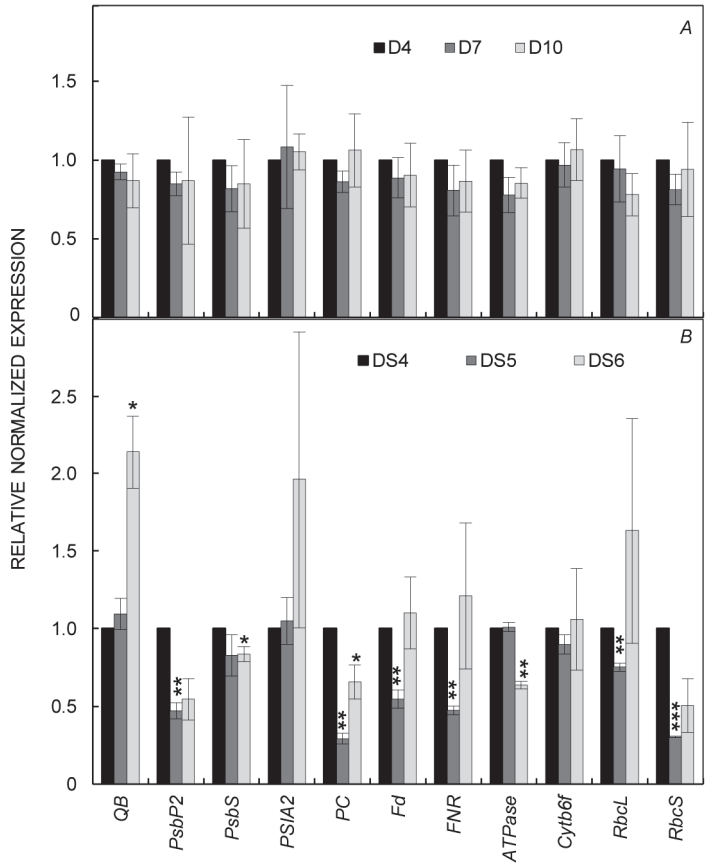

Fig. 5. Relative expression of genes analyzed by real-time RT-PCR in Pinot noir (*A*) leaf and (*B*) flower. In flower, measurements were performed at BBCH 57 (DS4), 60 (DS5), and 68 (DS6) stages. Six-week-old leaves were used and measurements were performed after four days (D4), seven (D7), and ten days (D10). Results represent the mean fold increase of mRNA over the first point of kinetics referred to as the 1x expression level: D4 for the leaves and DS4 for the flowers. Relative transcript accumulations of mRNA for each target gene in the flower at DS4 stage compared to leaves at D4 stage, referred to as the 1x expression level, were: 0.01 (*QB*), 0.23 (*PsbP2*), 0.11 (*PsbS*), 0.08 (*PSIA2*), 0.12 (*PC*), 0.10 (*Fd*), 0.06 (*FNR*), 0.95 (*ATPase*), 0.66 (*Cytb$_6$f*), 0.06 (*RbcL*), 0.07 (*RbcS*). The values significantly different from the first point of kinetics were marked by asterisks. The mean ± SE was calculated from three independent experiments.

promote ATP synthesis (Abdel-Reheem *et al*. 1991, Heber and Walker 1992, Bendall and Manasse 1995) and the recovery of PSII (Allakhverdiev *et al*. 2005).

The most striking results of this work were the CEF activation during inflorescence development. Today, it is relatively accepted that CEF occurs as a normal part of photosynthesis in leaf. CEF and LEF share a number of common carriers from PQ to Fd, nevertheless, the exact electron path and the regulation of this flow remain unclear. Breyton *et al*. (2006) have demonstrated the existence of a dynamic model for the occurrence of LEF and CEF in C_3 plants based on the competition between cyt b_6f and FNR for electrons carried by Fd. Indeed, once a reducing equivalent is generated at the reducing side of PSI, its involvement in either linear or cyclic flow is determined at the level of the Fd pool. Its oxidation by FNR and the $NADP^+$ pool would lead to LEF, while interaction with a putative Fd oxidizing site localized on the stromal side of cyt b_6f would initiate CEF. The latter might be mediated by a FNR molecule bound to cyt b_6f. Our results showed a reduction in flower FNR transcripts at DS5 which might be correlated with the induction of CEF at DS6 (Figs. 4*A*, 5*B*). Nevertheless, besides Fd and FNR pools, the redox state and activities are crucial in determining the fate of electrons from PSI (Breyton *et al*. 2006).

Several other possible CEF activators have been proposed, including the ATP/ADP ratio (Joliot and Joliot 2002), Calvin–Benson cycle intermediates or the reactive oxygen species, H_2O_2 (Gambarova 2008). Livingston *et al*. (2010) assumed the existence of a regulator (activator or inhibitor) of CEF, but no single metabolite appears to follow this pattern except RuBP.

This study clearly highlighted the differences between inflorescence and leaf in terms of photosynthetic activity and photochemical reaction regulations. Not surprisingly, leaf is the major photosynthetic organ and our results revealed that protective regulatory mechanisms of the photosynthetic chain were more efficient in this organ. More interestingly, our results showed that photosynthetic chain activity in inflorescence was particularly important during the first development stages which consolidate the assumption that young inflorescence (until the beginning of the flowering process) is implied in the whole carbon balance of grapevine plant. Our results also suppose that the inflorescence photosynthetic activity could be dissimulated by an intense respiratory activity.

Higher plants have complex and diverse set of mechanisms to regulate their photosynthetic electron transport including both rapid mechanisms, and long-term responses. The various modes of photosynthetic electron transport must be regulated in response to cell metabolic needs and regulations are needed to protect the organism from the destructive side-effects of light and redox reactions. We highlighted the activation of CEF in parallel to the decrease in LEF during inflorescence development. Therefore it is possible that in this organ, the cyclic electron flow is activated for the ATP requirement and reducing equivalents. Nevertheless, according to our results, it is also possible that the inflorescence develops an energy dissipating function, protection, and repair mechanism in order to prevent photodamage and to maintain the physiological integrity of photosynthetic apparatus.

References

Abdel-Reheem S., Belal M.H., Gupta G.: Photosynthesis inhibition of soybean leaves by insecticides. – Environ. Pollut. **74**: 245-250, 1991.

Allakhverdiev S.I., Nishiyama Y., Takahashi S. *et al*.: Systematic analysis of the relation of electron transport and ATP synthesis to the photodamage and repair of photosystem II in *Synechocystis*. – Plant Physiol. **137**: 263-273, 2005.

Antlfinger A., Wendel L.: Reproductive effort and floral photosynthesis in *Spiranthes cernua* (Orchidaceae). – Am. J. Bot. **84**: 769, 1997.

Aschan G., Pfanz H.: Non-foliar photosynthesis – a strategy of additional carbon acquisition. – Flora **198**: 81-97, 2003.

Avenson T.J., Cruz J.A., Kanazawa A. *et al*.: Regulating the proton budget of higher plant photosynthesis. – P. Natl. Acad. Sci. USA **102**: 9709-9713, 2005.

Bazzaz F.A., Carlson R.W., Harper J.L.: Contribution to reproductive effort by photosynthesis of flowers and fruits. – Nature **279**: 554-555, 1979.

Bendall D.S., Manasse R.S.: Cyclic photophosphorylation and electron transport. – BBA-Bioenergetics **1229**: 23-38, 1995.

Bertamini M., Muthuchelian K., Rubinigg M. *et al*.: Photoinhibition of photosynthesis in leaves of grapevine (*Vitis vinifera* L. cv. Riesling). Effect of chilling nights. – Photosynthetica **43**: 551-557, 2005.

Bertamini M., Nedunchezhian N.: Photoinhibition of photosynthesis in *Vitis berlandieri* and *Vitis rupestris* leaves under field conditions. – Photosynthetica **40**: 597-603, 2002.

Blanke M.M., Lenz F.: Fruit photosynthesis. – Plant Cell Environ. **12**: 31-46, 1989.

Breyton C., Nandha B., Johnson G.N. *et al*.: Redox modulation of cyclic electron flow around photosystem I in C_3 plants. – Biochemistry **45**: 13465-13475, 2006.

Carpentier R., Larue B., Leblanc R.M.: Photoacoustic spectroscopy of *Anacystis nidulans*: III. Detection of photosynthetic activities. – Arch. Biochem. Biophys. **228**: 534-543, 1984.

Carrara S., Pardossi A., Soldatini G. *et al*.: Photosynthetic activity of ripening tomato fruit. – Photosynthetica **39**: 75-78, 2001.

Clément C., Mischler P., Burrus M. *et al*.: Characteristics of the photosynthetic apparatus and CO_2-fixation in the flower bud of *Lilium*. II. Anther. – Int. J. Plant Sci. **158**: 801-810, 1997a.

Clément C., Mischler P., Burrus M. *et al*.: Characteristics of the photosynthetic apparatus and CO_2-fixation in the flower bud of *Lilium*. I. Corolla. – Int. J. Plant Sci. **158**: 794-800, 1997b.

Dogane Y., Ando T.: An estimation of carbon evolution during flowering and capsule development in a *Laeliocattleya* orchid. – Sci. Hortic.-Amsterdam **42**: 339-349, 1990.

Dueker J., Arditti J.: Photosynthetic CO_2 fixation by Green *Cymbidium* (Orchidaceae) flowers. – Plant Physiol. **43**:

130-132, 1968.
Finazzi G., Rappaport F., Furia A. *et al*.: Involvement of state transitions in the switch between linear and cyclic electron flow in *Chlamydomonas reinhardtii*. – EMBO Rep. **3**: 280-285, 2002.
Gambarova N.G.: Activity of photochemical reactions and accumulation of hydrogen peroxide in chloroplasts under stress conditions. – Russ. Agric. Sci. **34**: 149-151, 2008.
Genty B., Briantais J.M., Baker N.R.: The relationship between the quantum yield of photosynthetic electron transport and quenching of chlorophyll fluorescence. – Biochim. Biophys. Acta **990**: 87-92, 1989.
Golbeck J.H.: Structure, function and organization of the Photosystem I reaction center complex. – BBA-Bioeneretics **895**: 167-204, 1987.
Golbeck J.H., Bryant D.A.: Photosystem I. – Curr. Top. Bioenerg. **16**: 83-177, 1991.
Heber U., Walker D.: Concerning a dual function of coupled cyclic electron transport in leaves. – Plant Physiol. **100**: 1621-1626, 1992.
Heilmeier H., Whale D.M.: Carbon dioxide assimilation in the flowerhead of *Arctium*. – Oecologia **73**: 109-115, 1987.
Huang W., Zhang S.B., Cao K.F.: Stimulation of cyclic electron flow during recovery after chilling-induced photoinhibition of PSII. – Plant Cell Physiol. **51**: 1922-1928, 2010.
Huang W., Zhang S.B, Cao K.F.: Cyclic electron flow plays an important role in photoprotection of tropical trees illuminated at temporal chilling temperature. – Plant Cell Physiol. **52**: 297-305, 2011.
Jia H., Oguchi R., Hope A.B. *et al*.: Differential effects of severe water stress on linear and cyclic electron fluxes through Photosystem I in spinach leaf discs in CO_2-enriched air. – Planta **228**: 803-812, 2008.
Joët T., Cournac L., Peltier G. *et al*.: Cyclic electron flow around photosystem I in C3 plants. *In vivo* control by the redox state of chloroplasts and involvement of the NADH-dehydrogenase complex. – Plant Physiol. **128**: 760-769, 2002.
Johnson G.N.: Physiology of PSI cyclic electron transport in higher plants. – BBA-Bioenergetics **1807**: 384-389, 2011.
Joliot P., Joliot A.: Cyclic electron transfer in plant leaf. – P. Natl. Acad. Sci. USA **99**: 10209-10214, 2002.
Jurik T.W.: Differential costs of sexual and vegetative reproduction in wild strawberry populations. – Oecologia **66**: 394-403, 1985.
Keijzer C.J., Willemse M.T.M.: Tissue interactions in the developing locule of *Gasteria verrucosa* during microsporogenesis. – Plant Biol. **37**: 493-508,1988.
Kirichenko E.B., Chernyad'ev I., Voronkova T.V. *et al*.: Activity of the photosynthesis apparatus in orchids during flowering. – Fiziol. Rastenii **36**: 710-716, 1989.
Kirichenko E., Krendeleva T., Kukarskikh G. *et al*.: Photochemical activities of anther and pericarp chloroplast of cereals. – Russ. J. Plant Physl+ **40**: 229-233, 1993.
Klughammer C., Schreiber U.: An improved method, using saturating light pulses, for the determination of photosystem I quantum yield *via* P700+-absorbance changes at 830 nm. – Planta **192**: 261-268, 1994.
Klughammer C., Schreiber U.: Complementary PS II quantum yields calculated from simple fluorescence parameters measured by PAM fluorometry and the Saturation Pulse method. – PAM Application Notes **1**: 27-35, 2008.
Kotakis C., Kyzeridou A., Manetas Y.: Photosynthetic electron flow during leaf senescence: Evidence for a preferential maintenance of photosystem I activity and increased cyclic electron flow. – Photosynthetica **52**: 413-420, 2014.
Kramer D.M., Johnson G., Kiirats O. *et al*.: New fluorescence parameters for the determination of QA redox state and excitation energy fluxes. – Photosynth. Res. **79**: 209-218, 2004.
Kubicki A., Funk E., Westhoff P. *et al*.: Differential expression of plastome-encoded *ndh* genes in mesophyll and bundle-sheath chloroplasts of the C4 plant *Sorghum bicolor* indicates that the complex I-homologous NAD(P)H-plastoquinone oxidoreductase is involved in cyclic electron transport. – Planta **199**: 276-281, 1996.
Laisk A., Talts E., Oja V. *et al*.: Fast cyclic electron transport around photosystem I in leaves under far-red light: a proton-uncoupled pathway? – Photosynth. Res. **103**: 79-95, 2010.
Lebon G., Brun O., Magné C. *et al*.: Photosynthesis of the grapevine (*Vitis vinifera* L.) inflorescence. – Tree Physiol. **25**: 633-639, 2005a.
Lebon G., Duchêne E., Brun O. *et al*.: Flower abscission and inflorescence carbohydrates in sensitive and non-sensitive cultivars of grapevine. – Sex. Plant Reprod. **17**: 71-79, 2004.
Lebon G., Duchêne E., Brun O. *et al*.: Phenology of flowering and starch accumulation in grape (*Vitis vinifera* L.) cuttings and vines. – Ann. Bot.-London **95**: 943-948, 2005b.
Lebon G., Wojnarowiez G., Holzapfel B. *et al*.: Sugars and flowering in the grapevine (*Vitis vinifera* L.). – J. Exp. Bot. **59**: 2565-2578, 2008.
Livak K.J, Schmittgen T.D.: Analysis of relative gene expression using real-time quantitative PCR and the $2^{-\Delta\Delta C_T}$ method. – Methods **25**: 402-408, 2001.
Livingston A.K., Kanazawa A., Cruz J.A. *et al*.: Regulation of cyclic electron flow in C3 plants: differential effects of limiting photosynthesis at ribulose-1,5-bisphosphate carboxylase/ oxygenase and glyceraldehyde-3-phosphate dehydrogenase. – Plant Cell Environ. **33**: 1779-1788, 2010.
Marcelis L.F.M., Hofman-Eijer L.R.B.: The contribution of fruit photosynthesis to the carbon requirement of cucumber fruits as affected by irradiance, temperature and ontogeny. – Physiol. Plantarum **93**: 476-483, 1995.
Meier U.: Grapevine. – In: Meier U. (ed.): Growth Stages of Mono- and Dicotyledonous Plants BBCH Monograph Federal Biological Research Centre for Agriculture and Forestry. Pp. 93-95. Blackwell Wissenschafts-Verlag, Berlin 2001.
Miyake C., Miyata M., Shinzaki Y. *et al*.: CO_2 response of cyclic electron flow around PSI (CEF-PSI) in tobacco leaves – relative electron fluxes through PSI and PSII determine the magnitude of non-photochemical quenching (NPQ) of Chl fluorescence. – Plant Cell Physiol. **46**: 629-637, 2005.
Munekage Y., Hashimoto M., Miyake C. *et al*.: Cyclic electron flow around photosystem I is essential for photosynthesis. – Nature **429**: 579-582, 2004.
Munekage Y., Hojo M., Meurer J. *et al*.: *PGR5* is involved in cyclic electron flow around photosystem I and is essential for photoprotection in *Arabidopsis*. – Cell **110**: 361-371, 2002.
Nandha B., Finazzi G., Joliot P. *et al*.: The role of PGR5 in the redox poising of photosynthetic electron transport. – BBA-Bioenergetics **1767**: 1252-1259, 2007.
Palliotti A., Cartechini A.: Developmental changes in gas exchange activity in flowers, berries, and tendrils of field-grown Cabernet Sauvignon. – Am. J. Enol.Viticult. **52**: 317-323, 2001.
Petit A.-N., Baillieul F., Vaillant-Gaveau N. *et al*.: Low responsiveness of grapevine flowers and berries at fruit set to UV-C irradiation. – J. Exp. Bot. **60**: 1155-1162, 2009.

Reekie E.G., Bazzaz F.A.: Reproductive effort in plants. I. Carbon allocation to reproduction. – Am. Nat. **129**: 876-896, 1987.

Sawicki M., Aït Barka E., Clément C. *et al*.: Cross-talk between environmental stresses and plant metabolism during reproductive organ abscission. – J. Exp. Bot. **66**: 1707-1719, 2015a.

Sawicki M., Jeanson E., Celiz V. *et al*.: Adaptation of grapevine flowers to cold involves different mechanisms depending on stress intensity. – PLoS ONE **7**: e46976, 2012.

Sawicki M., Jacquens L., Baillieul F. *et al*.: Distinct regulation in inflorescence carbohydrate metabolism according to grapevine cultivars during floral development. – Physiol. Plantarum **154**: 447-467, 2015b.

Sawicki M., Aït Barka E., Clément C. *et al*.: Cold-night responses in grapevine inflorescences. – Plant Sci. **239**: 115-127, 2015c.

Schreiber U., Bilger W., Neubauer C.: Chlorophyll fluorescence as a nonintrusive indicator for rapid assessment of *in vivo* photosynthesis. – In: Schulze E..D, Caldwell M.M. (ed.): Ecophysiology of Photosynthesis. Pp. 49-70. Springer, Berlin Heidelberg 1994.

Shikanai T.: Central role of cyclic electron transport around photosystem I in the regulation of photosynthesis. – Curr. Opin. Biotech. **26**: 25-30, 2014.

Sonoike K.: Selective photoinhibition of photosystem I in isolated thylakoid membranes from cucumber and spinach. – Plant Cell Physiol. **36**: 825-830, 1995.

Takahashi S., Milward S.E., Fan D.Y. *et al*.: How does cyclic electron flow alleviate photoinhibition in *Arabidopsis*? – Plant Physiol. **149**: 1560-1567, 2009.

Vaillant-Gaveau N., Maillard P., Wojnarowiez G. *et al*.: Inflorescence of grapevine (*Vitis vinifera* L.): a high ability to distribute its own assimilates. – J. Exp. Bot. **62**: 4183-4190, 2011.

Vemmos S., Goldwin G.: The photosynthetic activity of Cox's Orange Pippin apple flowers in relation to fruit setting. – Ann. Bot.-London **73**: 385-391, 1994.

von Caemmerer S., Farquhar G.: Some relationships between the biochemistry of photosynthesis and the gas exchange of leaves. – Planta **153**: 376-387, 1981.

Weiss D., Shomer-Ilan A., Vainstein A. *et al*.: Photosynthetic carbon fixation in the corollas of *Petunia hybrida*. – Physiol. Plantarum **78**: 345-350, 1990.

Weiss D., Schönfeld M., Halevy A.H.: Photosynthetic activities in the *Petunia* corolla. – Plant Physiol. **87**: 666-670, 1988.

Werk K.S., Ehleringer J.R.: Photosynthesis by flowers in *Encelia farinosa* and *Encelia californica* (*Asteraceae*). – Oecologia **57**: 311-315, 1983.

Yonemori K., Itai A., Nakano R. *et al*.: Role of calyx lobes in gas exchange and development of Persimmon fruit. – J. Am. Soc. Hortic. Sci. **121**: 676-679, 1996.

Zapata C., Deléens E., Chaillou S. *et al*.: Mobilisation and distribution of starch and total N in two grapevine cultivars differing in their susceptibility to shedding. – Funct. Plant Biol. **31**: 1127-1135, 2004a.

Zapata C., Deléens E., Chaillou S. *et al*.: Partitioning and mobilization of starch and N reserves in grapevine (*Vitis vinifera* L.). – J. Plant Physiol. **161**: 1031-1040, 2004b.